J Electroceram (2012) 29:225–234
DOI 10.1007/s10832-012-9767-7

Fabrication and characterization of PZT (lead zirconate titanate) bridge-shaped resonator for mass sensing application

Dong Gun Hwang · Youn Mee Chae · Kyo Seon Hwang · Ji Yoon Kang · Soo Hyun Lee

Received: 7 August 2012 / Accepted: 1 October 2012 / Published online: 13 October 2012

Abstract Our research, based on executing theoretical modeling depending on the dimensions of PZT (lead zirconate titanate) thin film, was applied to two different bridge-shaped resonators. The critical point of having two different types of resonators is that it is a way of releasing the bridge. The first type of bridge-shaped resonator is released through use of an isotropic etching method using XeF_2 gas, while the second type of bridge-shaped resonator is released by a wet etching method that uses a KOH solution. The bridge-shaped resonators are anticipated to have accurate mass detecting sensors based on high mass sensitivity compared to the other shapes, such as diaphragms and cantilevers. The feasibility of a bridge-shaped PZT resonator as a mass sensor has been researched through studying the resonant frequency shift of a bridge-shaped resonator. The actual resonant properties of bridge-shaped resonators were determined by measuring resonant frequency and Q-factor measurements using an LDV (Laser Doppler Vibrometer). The resonant frequency appears in the ranges of 378.4–419.8, 144.0–180.3, and 107.8–123.4 kHz for dimensions of 50 μm×250 μm, 100 μm×500 μm, and 150 μm×750 μm, respectively. Finally, four different thicknesses of Titanium (Ti) were loaded on the bridge-shaped resonator to confirm its variation and mass sensitivity. Significantly, mass sensitivities with dimensions of 50 μm×250 μm, 100 μm×500 μm, and 150 μm×750 μm were 2.02 Hz/pg, 330.42 Hz/ng, and 43.67 Hz/ng, respectively. Thus, the bridge-shaped resonator with dimensions of 50 μm×250 μm was able to detect the picogram-level of a mass.

D. G. Hwang · Y. M. Chae · K. S. Hwang · J. Y. Kang · S. H. Lee (✉)
Center for BioMicrosystems,
Korea Institute of Science and Technology,
Seoul 136-791, Republic of Korea
e-mail: dream.ideal@gmail.com

Keywords PZT · Thin film · Bridge-shaped resonator · Mass sensor · Resonant frequency

1 Introduction

Mass measurements based on micro resonators or nano resonators have been the subject of growing interest over the last few years. The principle of operation is based on the detection of the shift of resonance frequency when a small quantity of mass is deposited on the sensing area [1]. This principle is applied to the recently developed resonators, which are used as biosensors to detect DNA [2] or RNA [3], antibodies and antigens [4–6], and the weights of cells [7]. Generally, the smaller the resonator, the more sensitive it is because the relative change of mass is greater. The silicon-based resonators have been the most actively researched due to their availability and easy integration with silicon-based technology. However, silicon-based resonators require an expensive optical apparatus because they cannot acquire a direct electrical signal [6]. In addition, there are generally optical limitations, such as a narrow dynamic range and parasitic deflection in optical measurements. Also, silicon-based resonators are measurable in high vacuum state [7]. To overcome the disadvantages of silicon-based resonators, a micro-resonator using PZT (lead zirconate titanate), a piezoelectric material, has been the subject of recent research efforts. A resonator using PZT is capable of driving and sensing mechanical resonance electrically due to its piezoelectric characteristic [6]. In addition, PZT resonators, unlike silicon-based resonators, do not require a high actuation voltage. Also, the high actuating characteristics of PZT make detection possible at room temperature and atmospheric pressure. In addition, it can be combined with CMOS

(complementary metal-oxide-semiconductor) technology to fabricate monolithic, integrated microsystems, allowing the assembly of arrays and matrices of resonators.

Generally, PZT resonators that can be utilized as mass sensors can be classified into three categories depending on their shape, i.e., diaphragm, cantilever, and bridge [8, 9]. A typical example for the diaphragm-shaped resonator is a quartz-crystal micro-balance (QCM). The advantages of the QCM include good frequency stability and reproducibility for detecting target materials. However, the QCM is not easy to integrate with other components as a sensor, and it is not compatible with the process for MEMS (micro-electro-mechanical systems) fabrication or conventional semiconductor fabrication because of its material properties. Also, QCM has a low sensitivity to mass change because of its relatively low operating frequency. Overall, QCM is impracticable for miniaturization [10]. To overcome the disadvantages of QCM, a diaphragm-shaped resonator using PZT has been researched, but this resonator still causes low mass sensitivity because of its shape compared to cantilever and bridge-shaped resonator.

In the case of a cantilever that is representative as a resonator, one side of the cantilever has a fixed end, while the other side has a free-standing end. When small particles are deposited on the cantilever, they alter the effective mass, causing a shift in the resonance frequency [11, 12]. In addition, the adhesion of target materials onto a cantilever induces changes in the surface stress and also shifts the resonance frequency [13]. It is still a matter of debate whether one is more dominant than the other in terms of a shift in the resonance frequency. To overcome the defects of the cantilever, a bridge-shaped resonator clamped on both sides was investigated in this research. If resonators for mass sensing are assumed to have the same geometrical conditions, i.e., length, width, and height, and the same mass of target material is applied to three different types of resonators (diaphragm, cantilever, and bridge-shaped), then a bridge-shaped resonator has excellent mass sensitivity compared to the other resonators [14, 15]. Accordingly, in the case of bridge-shaped resonators using PZT, they are expected to have accurate mass detecting sensors based on their high mass sensitivity.

In this paper, the possibility of a practical use of the bridge-shaped PZT resonator as a mass sensor has been researched through the resonant frequency shift of a bridge-shaped resonator. The resonant properties of a bridge-shaped resonator, on which a 1 μm PZT thin film had been deposited, were analyzed by theoretical modeling, depending on the dimensions of the bridge-shaped resonators. Based on this analysis, two different types of bridge-shaped resonators were fabricated. The critical point of having two different types of resonators is the manner for releasing the bridge. The first type of bridge-shaped resonator is released using an isotropic etching method using XeF_2 gas, while the second type of bridge-shaped resonator is released using the wet etching method with a KOH solution. The actual resonant properties of bridge-shaped resonators were determined through resonant frequency and Q-factor measurements using an LDV (Laser Doppler Vibrometer). Finally, titanium (Ti) was loaded onto the bridge-shaped resonator to confirm its mass detection ability.

2 Design and theoretical analysis

2.1 Theoretical modeling of multi-layered bridge resonator

According to its structural characteristics, a bridge-shaped PZT resonator has a specific resonant frequency, which can be calculated through theoretical modeling. Thus, before fabricating resonators, it is reasonable to understand the resonant properties of a bridge-shaped resonator through theoretical modeling. The theoretical nth mode resonant frequency of bridge-shaped resonators can be calculated by applying the Euler-Bernoulli theory, as shown below:

$$f_n = \frac{\lambda_n^2}{2\pi}\frac{1}{L^2}\sqrt{\frac{EI}{\rho A}}, \tag{1}$$

where E is Young's modulus of material consisting of the bridge, I is the moment of inertia, ρ is the density of the material consisting of the bridge, A and L represent the cross-sectional area and length, respectively, EI is the flexural stiffness of the bridge, ρA is the effective mass per unit length of the bridge, and λ_n, as a dimensionless, nth-mode eigen value has its own value depending on n [16]. As shown in Fig. 1, a bridge-shaped resonator has PZT and four different materials that compose a multi-layered structure. Thus, an analysis of the resonant properties is needed to consider the characteristics of the individual material by using Eq. 1. The characteristics of the materials based on EI and ρA must be considered, and they can be expressed as follows [17]:

$$EI = \sum_{i=1}^{j} E_i I_i \tag{2}$$

$$\rho A = \sum_{i=1}^{j} \rho_i A_i \tag{3}$$

In both Eqs. 2 and 3, i refers to the orders of the thin film consisting of the bridge, and j refers to the number of these.

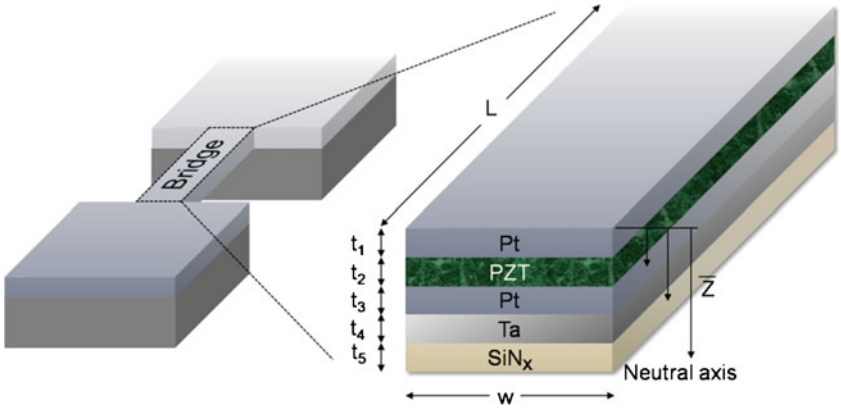

Fig. 1 Composition and materials of a bridge-shaped resonator

A neutral axis is considered to express the moment of inertia, I_i, of each thin film, and it is shown next (Steiner's law) [18].

$$Z = \frac{\sum_{i=1}^{j} E_i Z_i t_i}{\sum_{i=1}^{j} E_i t_i} \tag{4}$$

$$Z_i = \frac{\sum_{i=1}^{j} t_i}{2} \tag{5}$$

$$I_1 = \frac{1}{12} w t_1^3 + w t_1 (Z - Z_1)^2 \tag{6}$$

$$I_2 = \frac{1}{12} w t_2^3 + w t_2 (Z - Z_2)^2 \tag{7}$$

$$I_3 = \frac{1}{12} w t_3^3 + w t_2 (Z - Z_3)^2 \tag{8}$$

In Eqs. 4–8, z refers to the neutral axis of the bridge, and w and t refer to the width and the thickness of material of the bridge, respectively. In order to use Eqs. 2–8 to calculate the resonant frequency, the parameters shown in Table 1 must be available. Based on these parameters, the resonant frequencies of the bridge-shaped resonators can be calculated.

2.2 Theoretical analysis of resonant frequency with different dimensions

Resonant frequency has been theoretically analyzed based on the change of the dimensions in the multi-layer structure of the bridge-shaped resonator. The multi-layer structure is presumed to have a SiN_x/Ta/Pt/PZT/Pt structure, and the thicknesses are 1.0/0.03/0.15/1.0/0.1 μm, respectively. As shown in Fig. 2, the resonant frequency of the bridge that is 100 μm wide is analyzed based on the change in its length. As the length of the bridge increases, the resonant frequency decreases. As shown in Eq. 1, the resonant frequency is inversely proportional to the square of the length. On the other hand, a change in resonant frequency based on the change of the width of the bridge is not observed.

Table 1 Parameters of PZT, SiN_x, Ta, and Pt needed for the analytical calculation of a bridge-shaped resonator

Materials	Density, ρ (kg/m^3), ($\times 10^3$)	Young's modulus, E (N/m^2), ($\times 10^{10}$)	Thickness, t (m), ($\times 10^{-6}$)	Poison's ratio, ν
Pt	21.45	16.80	0.10	0.39
PZT	7.50	7.70	1.00	0.36
Ta	16.69	18.60	0.03	0.34
SiN_x	3.10	29.00	1.00	0.25

3 Experiments

3.1 Fabrication of PZT bridge-shaped resonator

As shown in Fig. 3, two different types of bridge-shaped resonators have been fabricated. In the first type, the width of the bridge is 50, 100, and 150 μm, and the length is 3, 5, and 10 times longer than the widths of the bridge, respectively. In addition, to release the bridge, the isotropic etching method using XeF_2 gas is used. In the second type of resonator, the width of the bridge is 50, 100, and 150 μm,

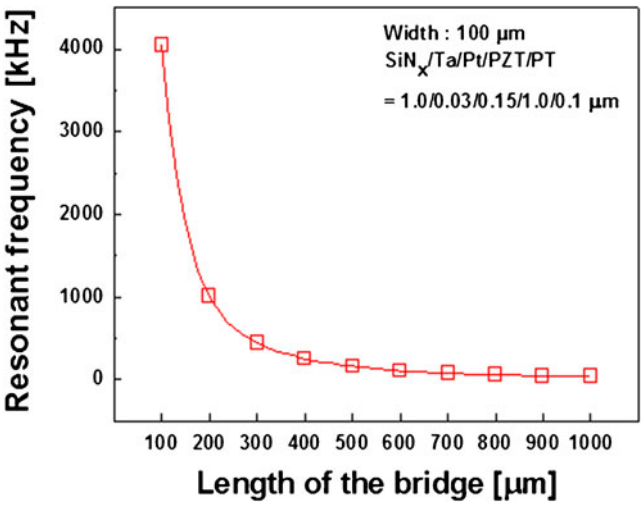

Fig. 2 Theoretical first mode resonant frequency based on length of the bridge

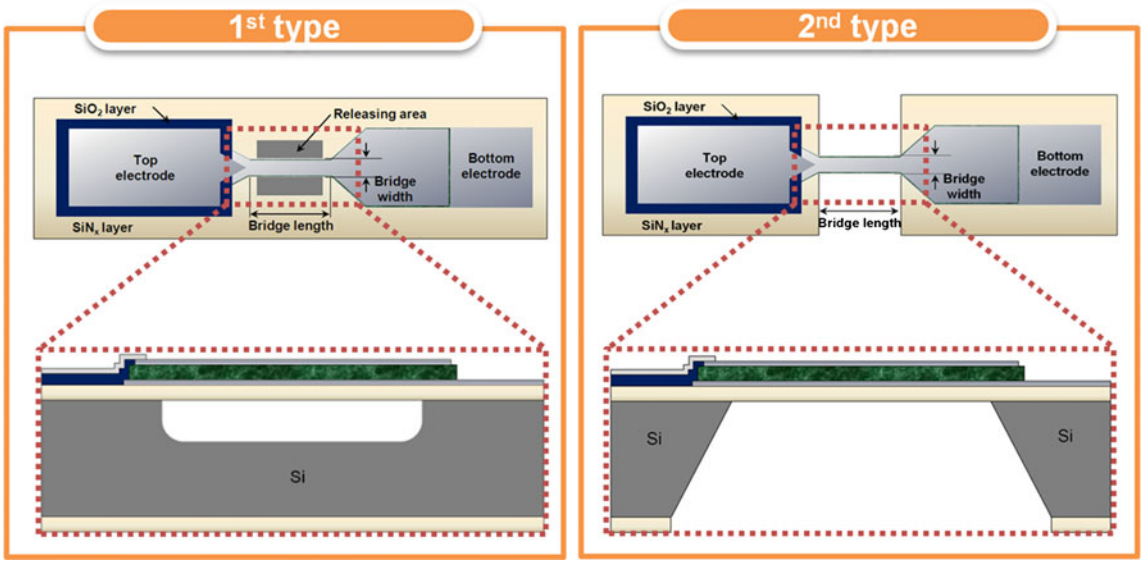

Fig. 3 Schematic images of first and second type bridge-shaped resonators based on different release methods

and the lengths are 5 times longer than the width of the bridge. Here, to release the bridge, the anisotropic Si bulk-etching method with KOH solution is used. The main difference between the first type and the second type is the manner in which the bridge is released. As a result, for the second type, extra photo-lithography is not required since the sensing area, on which the metal is deposited, is the backside of the bridge. It prevents any electrical shorts between the top electrode and the bottom electrode when metal is deposited on the surface of the bridge.

The procedure of fabricating a first type bridge-shaped resonator is shown in Fig. 4. By applying LPCVD (low pressure chemical vapor deposition), a 1 μm low-stress silicon nitride (SiN_x) thin film is deposited on a 4-inch silicon wafer. Then, a Pt layer as a bottom electrode with a thickness of 150 nm is deposited coming after Ta adhesive layer with a thickness of 30 nm by DC sputtering. PZT film manufactured by the diol-based sol-gel method is deposited with a thickness of 1 μm through the 12 times spin-coating method. Then, a Pt layer as a top electrode is deposited with a thickness of 100 nm through DC sputtering. Top Pt, PZT and bottom Pt layers are etched with the AOE (advanced oxide etcher) successively to shape the bridge. Also, bottom Pt remains partially as an electrical pad (Fig. 4(b)). With PECVD (plasma enhanced chemical vapor deposition), an SiO_2 layer is deposited with a thickness of 300 nm, and then it is etched partially using RIE (reactive ion etching) to make both an insulation layer and a buffer layer to compensate for

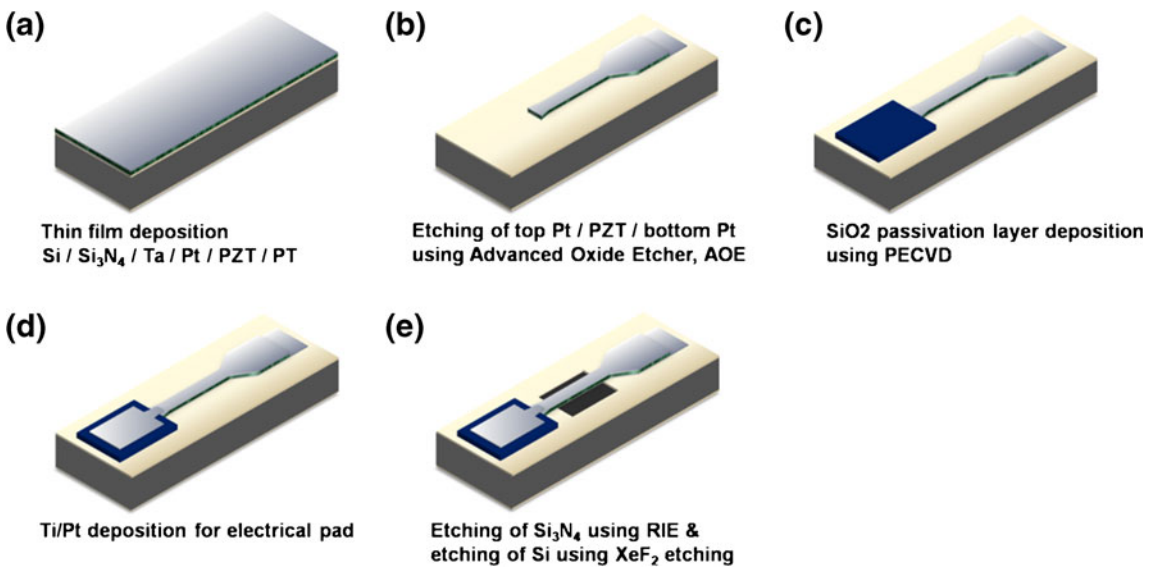

Fig. 4 Fabrication flow chart for a first type bridge-shaped resonator

the height difference (Fig. 4(c)). The lift-off method is used to deposit Ti/Pt (30 nm/300 nm) onto an aimed area of the SiO_2 layer. This process connects the electrical pad with the top Pt layer. For releasing the bridge, the SiN_x layer at the front side of the wafer is patterned with a photoresistor at both sides of the bridge and then etched using RIE. Finally, both sides of the Si are isotropically etched using XeF_2 gas. In Fig. 5, SEM images show the first type bridge-shaped resonators with dimensions of (a) 50 μm×250 μm, (b) 100 μm×500 μm, (c) 150 μm×750 μm, and (d) a multi-layered structure, respectively.

The fabrication flow chart of the second type bridge-shaped resonator is shown in Fig. 6. The fabrication process is the same as for the first type bridge-shaped resonator until just before the releasing process. In the second type, the SiN_x layer at the backside of the silicon wafer is patterned with a photoresistor and then etched using RIE. The bulk silicon is wet etched with a 30 % KOH solution. After the process is completed, the front of the SiN_x is removed using RIE, which completes the process for fabricating a second type bridge-shaped resonator.

In one completed wafer, there are 52 devices with the dimensions of 8 mm×12 mm. There are bridge arrays with the dimensions (W×L) of 50 μm×250 μm, 100 μm×500 μm, and 150 μm×750 μm. They are separated using a femtosecond laser micromachining workstation (MicroablaterTM M-2000, Exitech, Oerlikon Optics, Ltd., UK) to form a single device. In Fig. 7, SEM images show the second type bridge-shaped resonators with dimensions of (a) 50 μm×250 μm, (b) 100 μm×500 μm, (c) 150 μm×750 μm, and (d) a multi-layered structure, respectively.

3.2 Mass loading

The mass sensitivity of bridge-shaped resonators is evaluated by depositing Ti on the backside of the second type bridge-shaped resonators using an e-beam evaporator. To calculate the mass of Ti loaded onto the surface of the bridge-shaped resonators, the thickness monitor of the evaporator is used to observe the thickness of the deposited Ti. Thicknesses of 5, 10, 50, and 100 nm are

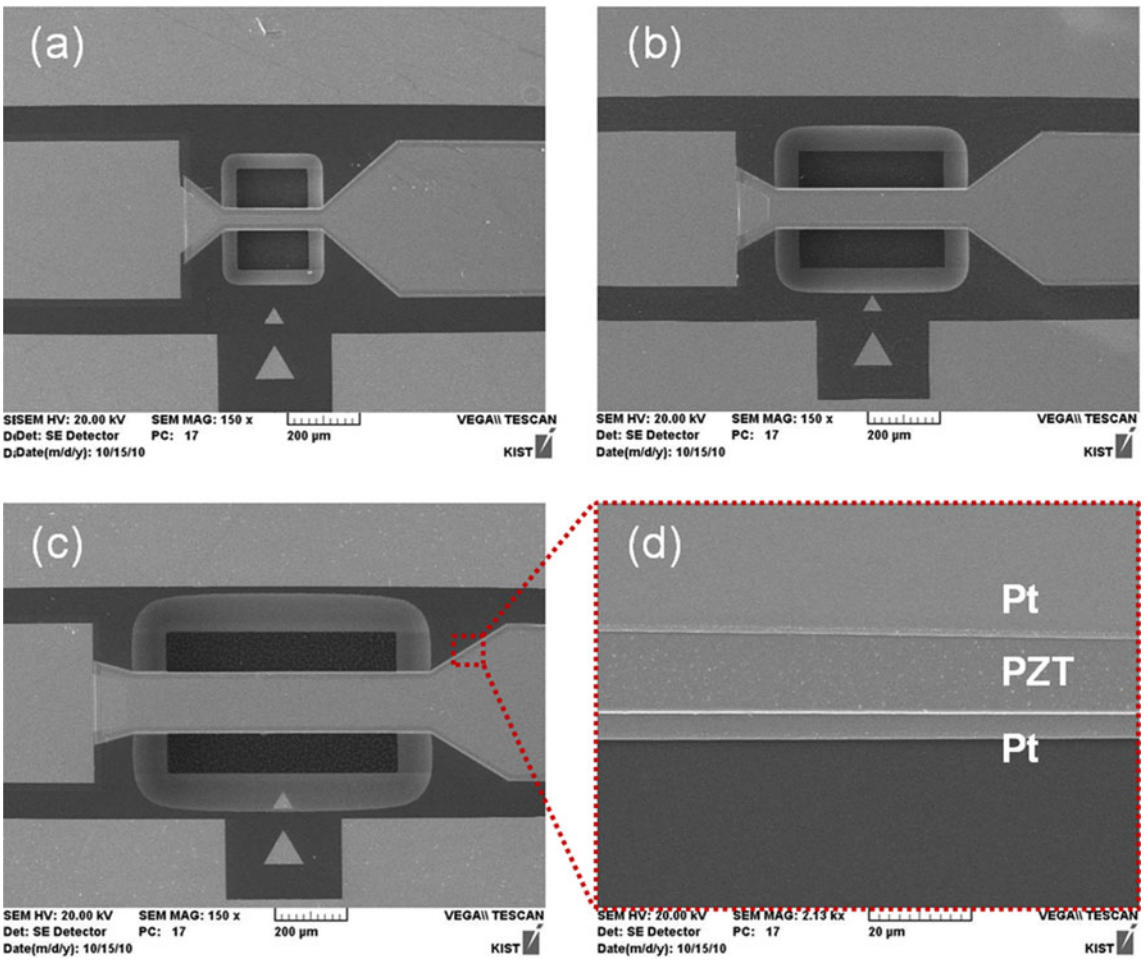

Fig. 5 SEM images of first type bridge-shaped resonators with dimensions of (**a**) 50 μm×250 μm, (**b**) 100 μm×500 μm, (**c**) 150 μm×750 μm and (**d**) their multi-layered structures, respectively

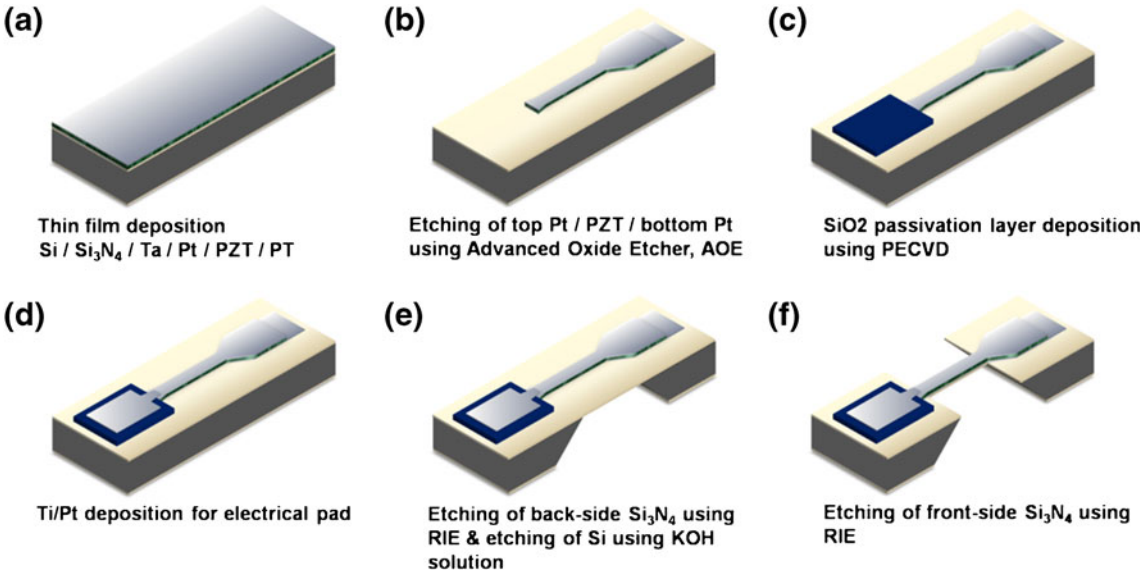

Fig. 6 Fabrication flow chart for a second type bridge-shaped resonator

deposited, and the mass is calculated using the density of Ti and the sensing area. Here, the density of Ti was 4.506 g/cm^3, while the mass calculated for each thickness is shown in Table 2.

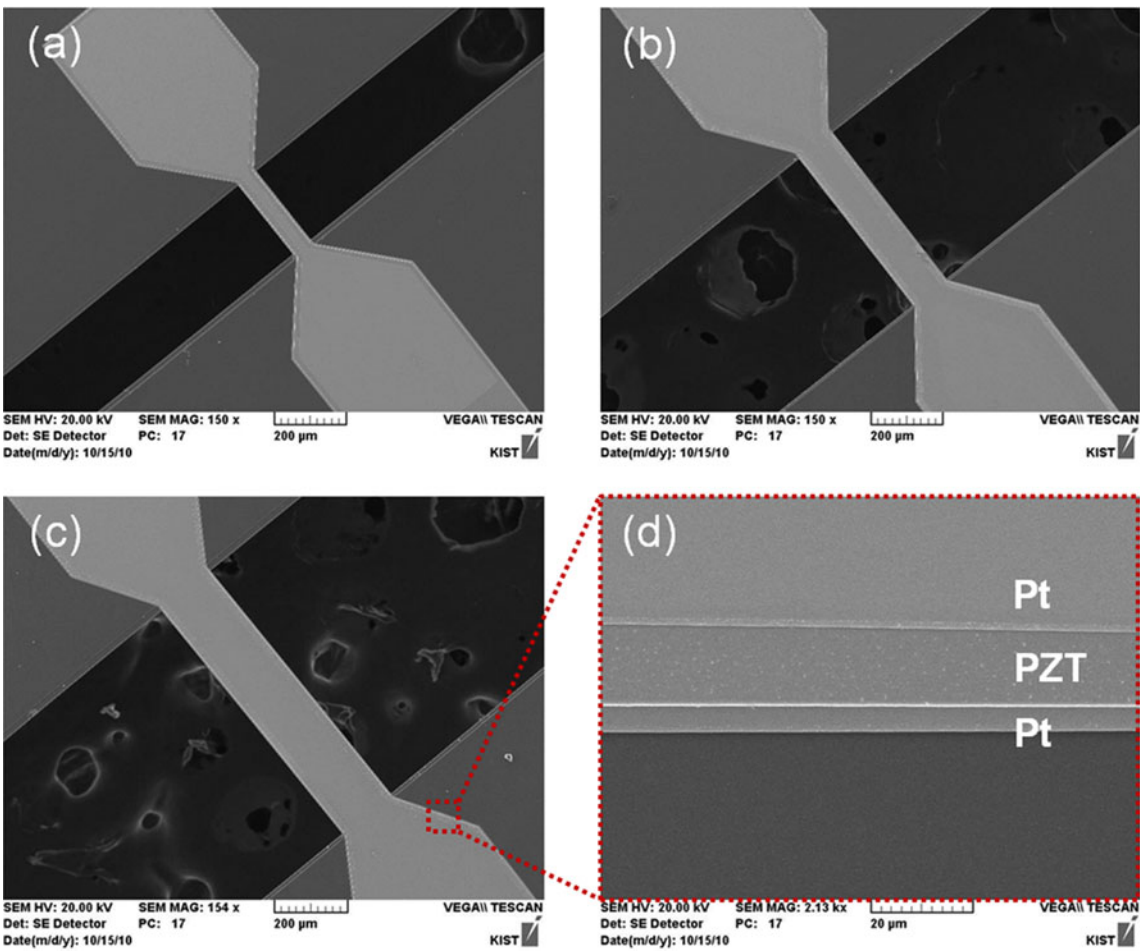

Fig. 7 SEM images of second type bridge-shaped resonators with dimensions of (**a**) 50 μm×250 μm, (**b**) 100 μm×500 μm, (**c**) 150 μm×750 μm and (**d**) their multi-layered structures, respectively

Table 2 Calculated Ti mass deposited on three different dimensions for four different Ti thicknesses

Bridge dimension	Ti mass (ng)				Sensing Area (μm^2)
	5 nm	10 nm	50 nm	100 nm	
50 μm×250 μm	0.28	0.56	2.81	5.63	12500
100 μm×500 μm	1.12	2.25	11.37	22.53	50000
150 μm×750 μm	2.53	5.07	25.35	50.69	112500

3.3 Resonant frequency measurements

The resonant frequency of the bridge-shaped resonators is measured using an optical heterodyne LDV (Laser Doppler Vibrometer) (MLD211D, Neo Ark Co. Japan) in an air environment. The experimental setup is shown in Fig. 8. A function waveform generator (33120A, Agilent) is used to generate 0.5 Vpp (peak-to-peak) sinusoidal wave forms, which are applied to the actuation (top) electrode while the bottom electrode is grounded. The vibration of the bridge-shaped resonators is measured with a vibrometer as sweeping sinusoidal wave forms in the designated range of frequency, and the means for finding the resonant frequency is chosen by finding the highest value of the vibration velocity. To confirm the mass sensitivity of the bridge-shaped resonators, the shift of the resonant frequency is also detected after the various thicknesses of Ti are deposited onto the resonator.

4 Results and discussion

4.1 Characterization of PZT bridge-shaped resonator with different dimensions

To discern the suitability of bridge-shaped resonators as mass sensors and to characterize their resonant properties, the resonant frequencies are measured and then the Q-factor is calculated based on the resonant frequency. The resonant frequency of the first type bridge-shaped resonator based on the ratio of width to length of the resonator is shown in Fig. 9. As described, as the length of the bridge increases, the resonant frequency decreases. Therefore, the experimental results correspond to Eq. 1, in which the resonant frequency is inversely proportional to the square of the length.

Based on the measured resonant frequency, the Q-factor is calculated as the ratio of width to length for the first type bridge-shaped resonator, as shown in Fig. 10. As a result, when the ratio of width to length is 1 to 5, the Q-factor has its highest value. A high Q-factor means that it will be easier to distinguish resonant frequency from non-resonant frequency. In view of the mass sensor, having a high Q-factor indicates improvement of resolution as a sensor. Therefore, when the ratio of width to length is 1 to 5, the bridge-shaped resonator is the most suitable as a mass sensor. This decision derives from considering both resolutions by Q-factor and mass sensitivity by the resonant frequency. When compromising both the high resonant frequency affects excellent

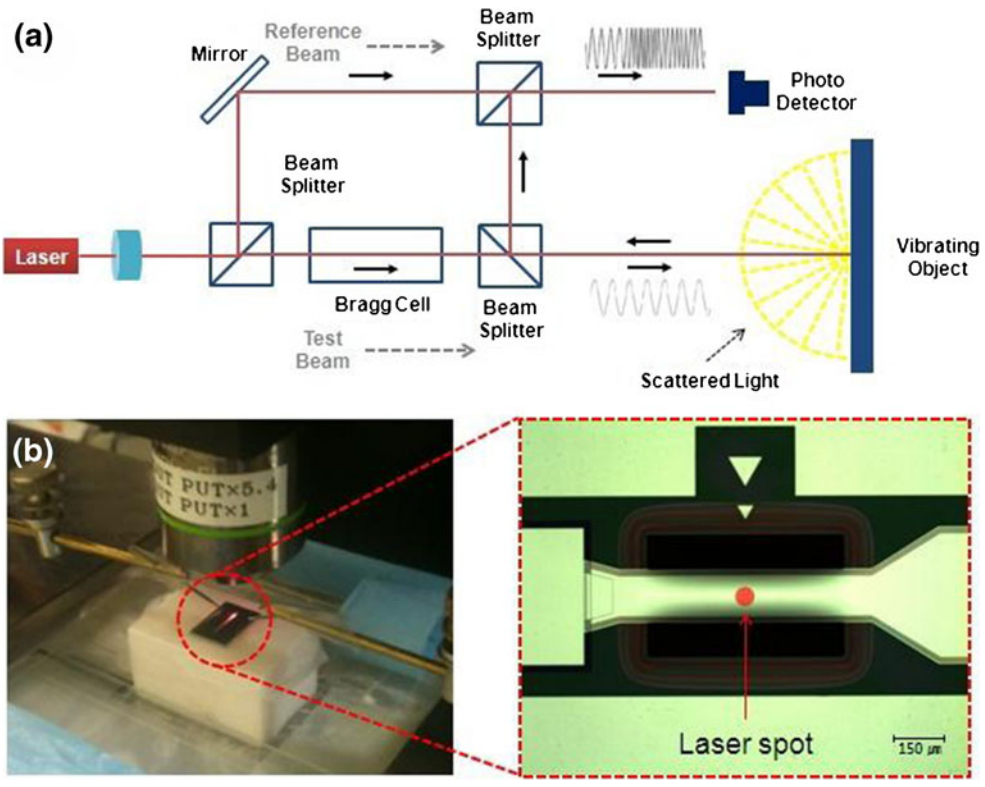

Fig. 8 Experimental set-up (**a**) a schematic for the operating principle of LDV system and (**b**) a laser spot on the bridge-shaped resonator

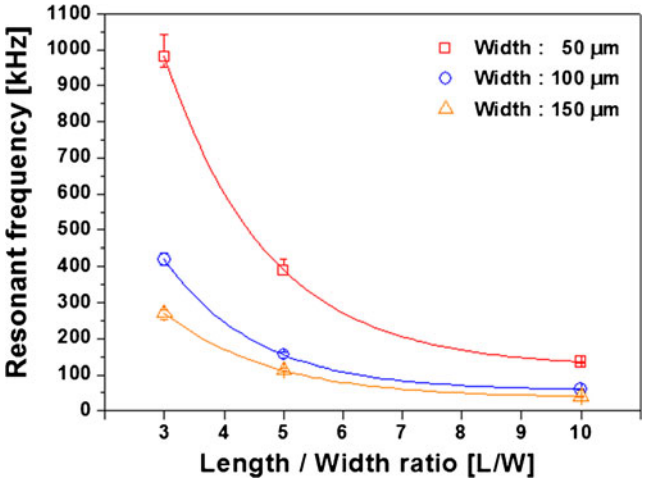

Fig. 9 Measured first resonant frequency as a function of the length/width ratio for the first type bridge-shaped resonators

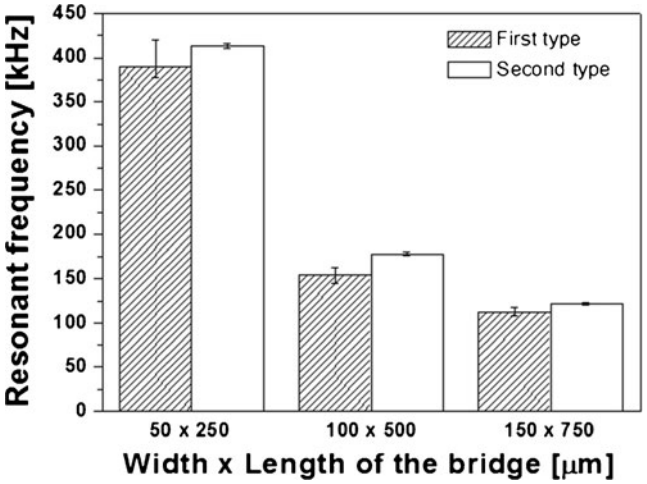

Fig. 11 Comparison of resonant frequency variations between first and second type bridge-shaped resonators

mass sensitivity and the high Q-factor affects excellent mass resolution, the bridge-shaped resonator with 1 to 5 ratio of width to length becomes the most suitable for the mass sensor.

From the considerations above, the second type bridge-shaped resonator having 1 to 5 ratio of width to length was fabricated and utilized as a mass sensor, making it possible to use the backside of the bridge for mass loading through metal deposition. Figure 11 shows the variation of the resonant frequency for the first and second type bridge-shaped resonators, respectively. The resonant frequencies were measured for 100 devices of each type and each dimension. In the case of a 50 μm×250 μm dimension, the first type bridge-shaped resonator shows about 11 % variation of the resonant frequency, while the second type bridge-shaped resonator shows less than 1 % variation of the resonant frequency. For other cases, they also show that the variation of the first type bridge-shaped resonator is much higher than that of the second type bridge-shaped resonator. Because the first type bridge-shaped resonator is released with XeF_2 gas, the isotropic etching degree varies by batch and causes the length of the bridge to be different. In case of the second type bridge-shaped resonator being released with the KOH wet etching method, the etching profile is constant and helps to keep the length of the bridge uniform. Therefore, second type bridge-shaped resonators have a variation within 1 % for the resonant frequencies of each device.

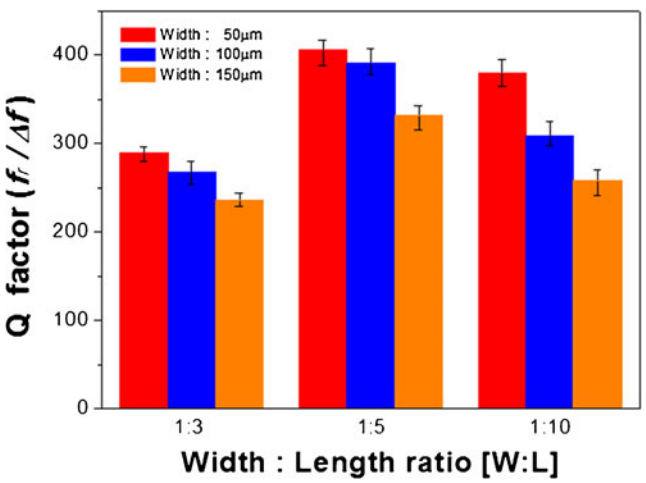

Fig. 10 Calculated Q-factors as a function of the width/length ratio for bridge-shaped resonators

4.2 Mass sensitivity

To see a shift of the resonant frequency according to the mass increase, the resonant frequency of the second type bridge-shaped resonator is observed when Ti is loaded with 10 nm thickness. These results are shown in Fig. 12. Devices with a dimension of 50 μm×250 μm, 100 μm×500 μm, and 150 μm×750 μm were used to detect the resonant frequency shift before and after Ti deposition. They showed that resonant frequency shifts toward the low range of the frequency are caused by mass loading. These results reflect that, in Eq. 1, the resonant frequency decreases when the mass increases.

Mass sensitivity is a very important characteristic when a bridge-shaped resonator is applied as a mass sensor. To confirm the mass sensitivity of the second type bridge-shaped resonators, a shift of the resonant frequency was measured for four different thicknesses of Ti deposited, i.e., 5, 10, 50, and 100 nm, as shown in Fig. 13. Each resonant frequency is the average value of 10 devices. As the mass of Ti deposited on the bridge increases, resonant frequency decreases linearly. Mass sensitivities ($S=\Delta f/\Delta m$) are calculated with the measured resonant frequency and the mass from Table 2. Mass sensitivities with dimensions of

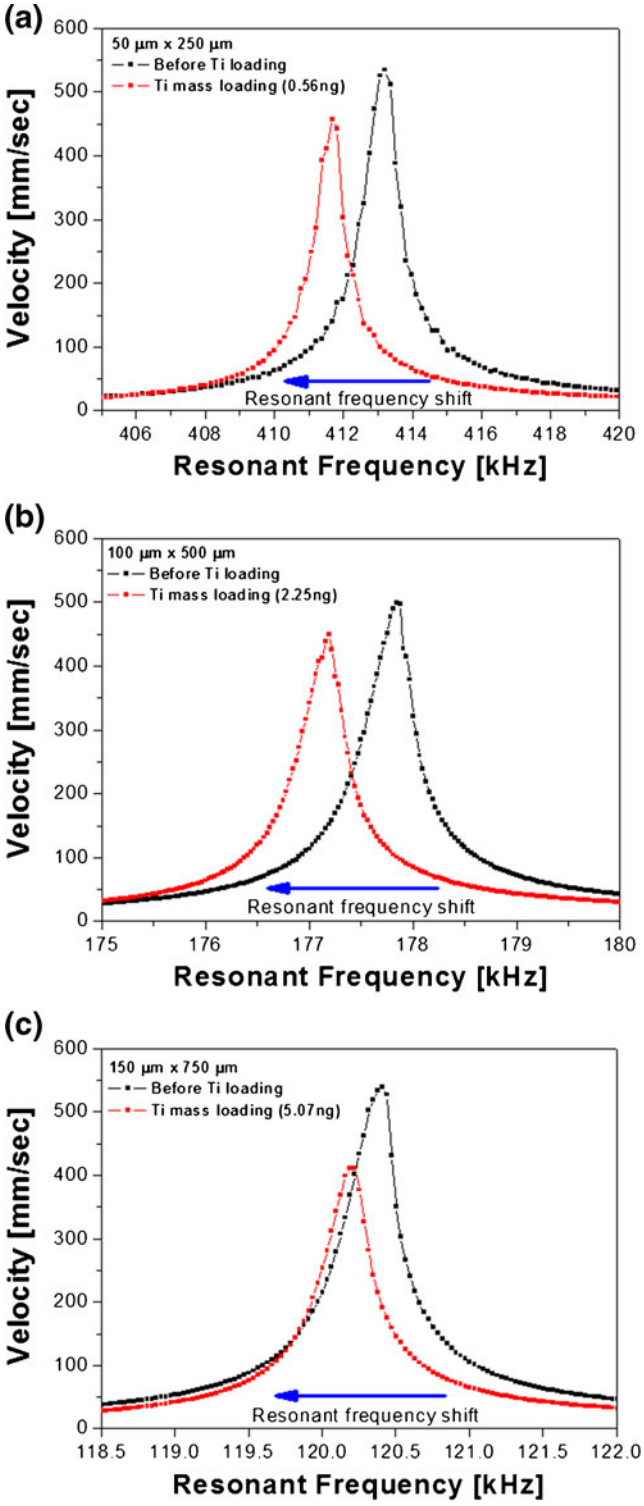

Fig. 12 Resonant frequency shift of second type bridge-shaped resonators after Ti mass loading: (**a**) 50 μm×250 μm, (**b**) 100 μm×500 μm, and (**c**) 150 μm×750 μm

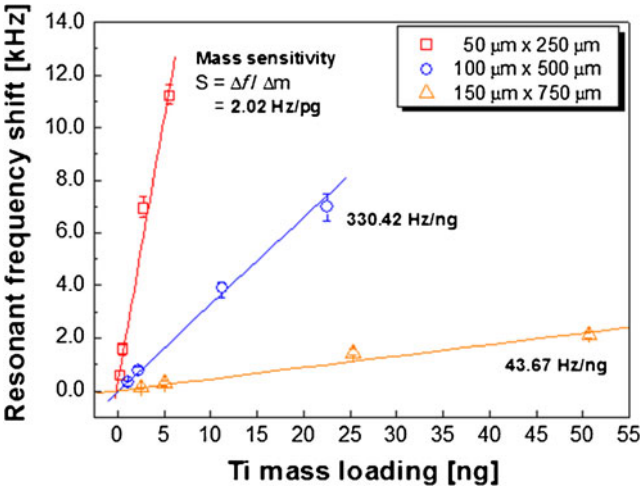

Fig. 13 Mass sensitivities of second type bridge-shaped resonators for different dimensions

50 μm×250 μm, 100 μm×500 μm, and 150 μm×750 μm were 2.02 Hz/pg, 330.42 Hz/ng, and 43.67 Hz/ng, respectively. That is, a smaller dimension of a bridge-shaped resonator leads to a bigger shift of resonant frequency with Ti mass loading. In the case of dimensions of 50 μm×250 μm, it was able to detect picogram levels of mass.

5 Conclusions

The feasibility of a PZT (lead zirconate titanate) bridge-shaped resonator as a mass sensor was researched through examining resonant frequency shift. The resonant properties of bridge-shaped resonators deposited with a 1.0 μm thickness of PZT thin film were analyzed using theoretical models that depended on their dimensions. Based on this analysis, two types of bridge-shaped resonators were fabricated with dimensions (W×L) of 50 μm×250 μm, 100 μm×500 μm, and 150 μm×750 μm. The first type bridge-shaped resonator was released with XeF_2 gas, and the second type bridge-shaped resonator was released using the KOH wet-etching method.

The actual resonant properties of bridge-shaped resonators were interpreted through resonant frequency measurement and calculation of Q-factor, using an LDV (Laser Doppler Vibrometer). Considering both high resonant frequency effects, i.e., excellent mass sensitivity and (high Q-factor effects) excellent mass resolution, the bridge-shaped resonator with a 1 to 5 ratio of width to length is the most suitable for a mass sensor. Further, in terms of the resonant frequency, the second type bridge-shaped resonators have a variation within 1 %, which is much less than that for the first type bridge-shaped resonator.

From these analyses, the second type bridge-shaped resonator with a 1 to 5 ratio of width to length was fabricated and utilized as a mass sensor to confirm its mass sensitivity. The smaller dimension of the bridge-shaped resonator leads to a larger shift of resonant frequency with Ti mass loading.

Also, with the dimensions of 50 μm×250 μm, it was able to detect the picogram levels of mass. In future work, we will try to develop this sensor as a biosensor to detect specific antigens in real time after integrating a microfluidic component.

Acknowledgments This research was partially supported by the Happy tech. program through the National Research Foundation of Korea (NRF) funded by the Ministry of Education, Science and Technology (grant number: 2009-0091918, 2010-0020786). And also, the authors are very grateful for the financial support from the KIST institutional program.

References

1. J. Arcamone, G. Rius, G. Abadal, J. Teva, N. Barniol, F. Pérez-Murano, Microelectron. Eng. **83**, 1216–1220 (2006)
2. B. Ilic, Y. Yang, K. Aubin, R. Reichenbach, S. Krylov, H.G. Craighead, Nano Lett.. **5**(5), 925–929 (2005)
3. J. Zhang, H.P. Lang, F. Huber, A. Bietsch, W. Grange, U. Certa, R. McKendry, H.J. Guntherodt, M. Hegner, C. Gerber, Nat. Nanotechnol. **1**(3), 214–220 (2006)
4. Y. Arntz, J.D. Seelig, H.P. Lang, J. Zhang, P. Hunziker, J.P. Ramseyer, E. Meyer, M. Hegner, G. Ch, Nanotechnology **14**(1), 86 (2003)
5. K.S. Hwang, J.H. Lee, J. Park, D.S. Yoon, J.H. Park, T.S. Kim, Lab Chip **4**(6), 547–552 (2004)
6. J.H. Lee, K.S. Hwang, J. Park, K.H. Yoon, D.S. Yoon, T.S. Kim, Biosens. Bioelectron. **20**(10), 2157–2162 (2005)
7. B. Ilic, D. Czaplewski, M. Zalalutdinov, H.G. Craighead, P. Neuzil, C. Campagnolo, C. Batt, J. Vac, Sci. Technol. B **19**, 2825–2828 (2001)
8. D. L. Polla, SPIE: Smart Structures and Materials 1997, **3046**, ed. by V. K. Varadan, P. J. McWhorter (SPIE-Int Soc Optical Engineering, San Diego, 1997), 24–27
9. L. Chengkuo, T. Itoh, T. Suga, IEEE T Ultrason Ferr **43**, 553–559 (1996)
10. T. Xu, Z. Wang, J. Miao, L. Yu, C.M. Li, Biosens. Bioelectron. **24** (4), 638–643 (2008)
11. B. Rogers, L. Manning, M. Jones, T. Sulchek, K. Murray, B. Beneschott, J.D. Adams, Z. Hu, T. Thundat, H. Cavazos, S.C. Minne, Rev. Sci. Instrum. **74**(11), 4899–4901 (2003)
12. E. Forsen, G. Abadal, S. Ghatnekar-Nilsson, J. Teva, J. Verd, R. Sandberg, W. Svendsen, F. Perez-Murano, J. Esteve, E. Figueras, F. Campabadal, L. Montelius, N. Barniol, A. Boisen, Appl. Phys. Lett. **87**(4), 043507–043503 (2005)
13. H.S. Tzou, H.J. Lee, S.M. Arnold, Mech. Adv. Mater. Struc. **11**(4–5), 367–393 (2004)
14. M. Zang, S. M. Zurn, D. L. Polla, B. J. Nelson, W. P. Robbins, MSM2000: Technical Proceedings, ed. by M. Laudon, B. Romanowicz (Computational Publications, San Diego, 2000), 265–268
15. S. Shin, N.-E. Lee, H.-D. Park, J.-S. Park, J. Lee, Integr. Ferroelectr. **80**(1), 355–362 (2006)
16. W. Weaver, S. Timoshenko, D.H. Young, *Vibration problems in engineering* (John Wiley & Sons, USA, 1990)
17. R.J. Roark, W.C. Young, *Formulas for stress and strain* (McGraw-Hill, USA, 1982)
18. V. Cimalla, F. Niebelschütz, K. Tonisch, C. Foerster, K. Brueckner, I. Cimalla, T. Friedrich, J. Pezoldt, R. Stephan, M. Hein, O. Ambacher, Sensor Actuat B-Chem **126**(1), 24–34 (2007)